BIOCHEMISTRY
including biophysical chemistry & molecular biology

Article

pubs.acs.org/biochemistry

Identification of Mitochondrial Electron Transport Chain-Mediated NADH Radical Formation by EPR Spin-Trapping Techniques

Satoshi Matsuzaki,[†] Yashige Kotake,[†] and Kenneth M. Humphries*[,†,‡,§]

[†]Free Radical Biology and Aging Research Program, Oklahoma Medical Research Foundation, Oklahoma City, Oklahoma 73104-5097, United States

[‡]Department of Biochemistry and Molecular Biology and [§]Reynolds Oklahoma Center on Aging, University of Oklahoma Health Sciences Center, Oklahoma City, Oklahoma 73117-1215, United States

ABSTRACT: The mitochondrial electron transport chain (ETC) is a major source of free radical production. However, due to the highly reactive nature of radical species and their short lifetimes, accurate detection and identification of these molecules in biological systems is challenging. The aim of this investigation was to determine the free radical species produced from the mitochondrial ETC by utilizing EPR spin-trapping techniques and the recently commercialized spin-trap, 5-(2,2-dimethyl-1,3-propoxycyclophosphoryl)-5-methyl-1-pyrroline *N*-oxide (CYPMPO). We demonstrate that this spin-trap has the preferential quality of having minimal mitochondrial toxicity at concentrations required for radical detection. In rat heart mitochondria and submitochondrial particles supplied with NADH, the major species detected under physiological pH was a carbon-centered radical adduct, indicated by markedly large hyperfine coupling constant with hydrogen (a_H > 2.0 mT). In the presence of the ETC inhibitors, the carbon-centered radical formation was increased and exhibited NADH concentration dependency. The same carbon-centered radical could also be produced with the NAD biosynthesis precursor, nicotinamide mononucleotide, in the presence of a catalytic amount of NADH. The results support the conclusion that the observed species is a complex I derived NADH radical. The formation of the NADH radical could be blocked by hydroxyl radical scavengers but not SOD. In vitro experiments confirmed that an NADH-radical is readily formed by hydroxyl radical but not superoxide anion, further implicating hydroxyl radical as an upstream mediator of NADH radical production. These findings demonstrate the identification of a novel mitochondrial radical species with potential physiological significance and highlight the diverse mechanisms and sites of production within the ETC.

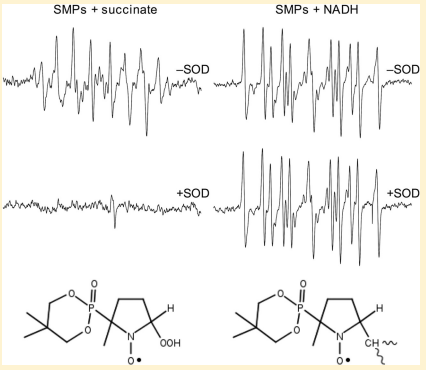

Superoxide anion has long been considered the primary free radical species produced by mitochondria. Nevertheless, the mitochondrial production of other species, including reactive oxygen, nitrogen, and carbon species, may also have significant biological functions. Such species may be significant contributors to oxidative damage and/or redox-based signaling. Recently, several lines of evidence indicated the possibility of mitochondrion-originated carbon-centered radicals, including lipid radicals,[1−5] semiquinone radicals,[6] and other, yet to be determined species.[7,8] Nevertheless, the origins and consequences of carbon-centered radical formation are not well-known. Because of the high reactivity of radical species, carbon-centered radicals can be postulated to be either products of upstream reactions, intermediate products of multielectron redox signaling, or reactants that promote the production of other reactive radical species.

The short lifetime of free radicals makes identification of species produced by mitochondria challenging, even with the use of electron paramagnetic resonance (EPR) spin-trapping techniques. This is, in part, because the lifetime of superoxide adducts (−OOH) is fairly short,[9] and the use of high concentrations of traditional spin-traps, such as DMPO, may directly inhibit mitochondrial function and cause either an over- or underestimation of free radical production.[10,11] Better identification of species may potentially be achieved by the use of probes that have a higher spin-trapping rate, thus necessitating a lower concentration of spin-trap needed for signal detection. A recently developed spin-trap 5-(2,2-dimethyl-1,3-propoxycyclophosphoryl)-5-methyl-1-pyrroline *N*-oxide (CYPMPO),[12] a cyclic DEPMPO-like nitrone trap, may provide new free radical information when used with mitochondria. As compared to DMPO, CYPMPO has a superior reaction rate toward oxygen free radicals and has longer half-lives for adducts.[11,12] Thus, the use of CYPMPO and the analysis of hyperfine coupling (HFC) constants for spin-adducts may offer a powerful tool for the identification of free radical species generated by mitochondria.

Complex I (NADH−ubiquinone oxidoreductase) of the electron transport chain (ETC) is one of the primary sites of free radical production in mitochondria.[13] Complex I contains several distinct moieties and sites that have been demonstrated

Received: November 15, 2011
Revised: November 16, 2011
Published: November 17, 2011

to be sources of free radicals, including flavin mononucleotide (FMN), iron−sulfur (Fe−S) clusters, and the ubiquinone binding site.[14] The production of free radicals from any or all of these sites is largely dictated by the energetic status.[14] In general, a site that is maintained in a more reduced state has a greater propensity to generate free radicals. While these redox centers are implicated sites of superoxide anion and hydroxyl radical production, their capacity to generate carbon-centered radicals and/or protein-centered radicals is not well-known. In this study, we have exploited the advantageous properties of CYPMPO to identify the formation of a complex I-mediated carbon-centered radical in isolated mitochondria. Characterization of the carbon-centered radical is consistent with an NADH radical species, which is produced in a complex I redox and hydroxyl radical dependent manner. Formation of this species is dictated by the mitochondrial NADH/NAD^+ ratio, thus providing critical insight into the metabolic conditions that may favor free radical production.

MATERIALS AND METHODS

Reagents and Animals. Antimycin A, glutamate, malate, malate dehydrogenase, NAD^+, NADH, nicotinamide mononucleotide (NMN), rotenone, succinate, and superoxide dismutase (CuZnSOD) were purchased from Sigma. Reduced nicotinamide mononucleotide (NMNH) was generated by reduction of 20 mM NMN with equimolar $NaBH_4$ and followed to completion by monitoring the increase in absorbance at 340 nm. 5-(2,2-Dimethyl-1,3-propoxycyclophosphoryl)-5-methyl-1-pyrroline *N*-oxide (CYPMPO, Figure 1) was purchased from Radical Research (Tokyo, Japan). DEPMPO, BMPO, CMH, and DMPO were purchased from Enzo Life Sciences. Male Sprague−Dawley rats (250−300 g) were obtained from Harlan Laboratories.

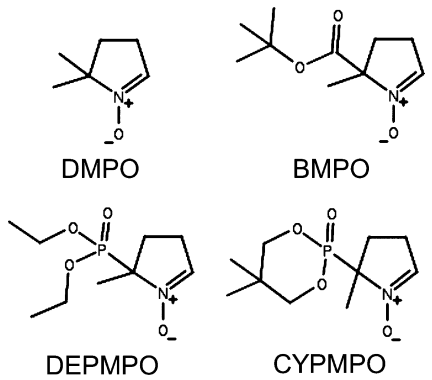

Figure 1. Chemical structures of DMPO, BMPO, DEPMPO, and CYPMPO.

Isolation of Cardiac Submitochondrial Particles (SMPs)/Mitoplasts and Assessment of Electron Transport Activity. SMPs and mitoplasts were isolated from hearts as previously described.[15] Briefly, Sprague−Dawley rats were euthanized by decapitation. Hearts were excised immediately and perfused with 10 mL of ice-cold isolation buffer [210 mM mannitol, 70 mM sucrose, 1.0 mM EDTA, and 10 mM MOPS (pH 7.4)] to remove blood. Hearts were then snap-frozen in liquid N_2 and pulverized. Pulverized tissue was placed into 20 mL of 10 mM MOPS and 1.0 mM EDTA (pH 7.4) and homogenized by 4 × 4 s passes using a Polytron homogenizer followed by 15 passes with a Potter-Elvejem homogenizer. Homogenate was then centrifuged at 750*g* for 5.0 min, and the supernatant was collected. The supernatant was centrifuged at 10000*g* for 20 min, and the resulting pellet, representing mitoplasts, was resuspended in 12 mL of 10 mM MOPS and 1.0 mM EDTA (pH 7.4) (2.0−5.0 mg/mL). Following two cycles of freezing (liquid N_2) and thawing, the solution was sonicated on ice (8 × 15 s with 30 s intervals, sonic dismembrator output of 20 W). The sonicated preparation was then centrifuged at 10000*g* for 7.0 min to remove unbroken mitoplasts. The supernatant was centrifuged at 40000*g* for 60 min. The resulting pellet, containing submitochondrial particles, was resuspended in 10 mM MOPS (pH 7.4) at a protein concentration of 1.0 mg/mL. NADH oxidase activity, an assessment of overall electron transport activity thru complexes I, III, and IV, was measured utilizing a multichannel transporter on an Agilent 8453 diode array UV−vis spectrophotometer. Activity was measured as the rate at which SMPs at 25 μg/mL oxidized 200 μM NADH (ε_{340} = 6200 M^{-1} cm^{-1}) in 10 mM MOPS (pH 7.4), 25 mM KCl, and 1 mM EDTA.

EPR Spin-Trapping Experiments. The EPR spectra were obtained by using a Bruker EMX spectrometer (Billerica, MA) operating at X-band (~9.78 GHz) with a 100 kHz modulation frequency and ER 41225SHQ high-sensitivity cavity. Typical settings for the spectrometer are: microwave power, 6.325 mW; modulation amplitude, 1.5 G; scan range, 150 G; time constant, 655 ms. The reaction mixtures indicated in the respective figure legends were assembled in microcentrifuge tubes, and after indicated incubation time the mixtures were transferred to a quartz flat cell for the EPR determination. Typical incubation times for SMPs/mitoplasts system were 30 min and for xanthine/xanthine oxidase system were 10 min. All the EPR experiments were performed in 10 mM MOPS (pH 7.4), 25 mM KCl, 1 mM EDTA, and 40 μM diethylenetriaminepentaacetic acid (DTPA), at room temperature. For the kinetics experiment shown in Figure 9B, the reaction mixtures were introduced to the flat cell immediately after the reaction was initiated, and 3 min incremental sweeps were performed. Similarly, for the CMH kinetics experiment shown in Figure 5, the reaction was initiated in the flat cell in the cavity and time-course (fixed-field) measurement was performed.

Statistical Analysis. Data are presented as means ± SD. The data were evaluated utilizing a two-tailed *t* test. Statistical significance was assigned for $p \leq 0.05$, as indicated.

Computer Simulations. Spectral simulations are performed using the WinSim 2002 computer program of NIEHS public EPR software tools packages.[16] The parameters that were used for simulating the experimental EPR spectra are described in the figure legends.

RESULTS

Characterization of the Spin-Trap CYPMPO. Initial experiments were undertaken to characterize the spin-adduct of CYPMPO using a well-established enzymatic superoxide generating system, xanthine and xanthine oxidase (X/XO). Figure 2 shows representative EPR spectra of CYPMPO−superoxide adduct (CYPMPO−OOH) and CYPMPO−hydroxyl radical adduct (CYPMPO−OH) derived from the X/XO system. As expected, the major product from the X/XO system was superoxide, and exogenously supplied SOD1 (CuZnSOD) specifically abolished the superoxide adduct peaks. Hyperfine coupling (HFC) constants used for the simulation are listed in the figure caption. These experiments employed the same

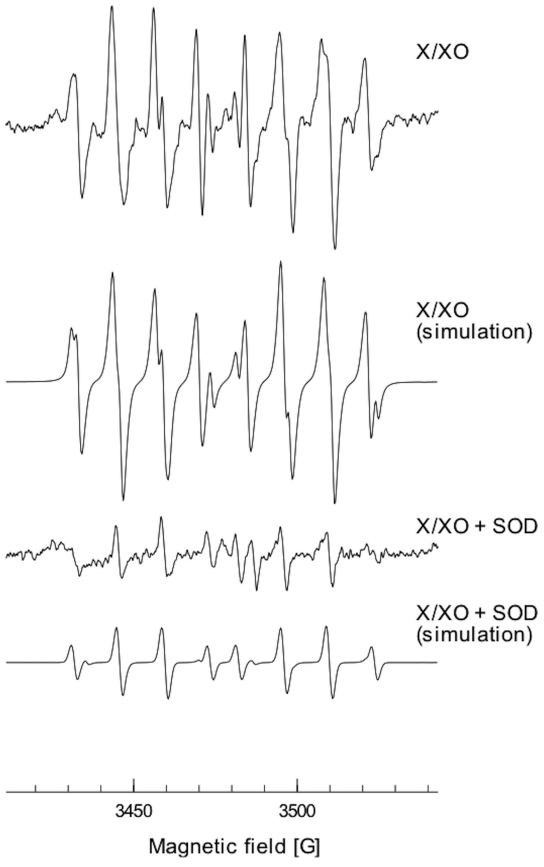

Figure 2. EPR spectra of CYPMPO−OOH and CYPMPO−OH adducts derived from xanthine/xanthine oxidase free radical generation system. CYPMPO (5 mM) was incubated with xanthine (5 mM) and xanthine oxidase (50 mU/mL) in 10 mM MOPS (pH 7.4), 1 mM EDTA, and 40 μM DTPA, in the absence or presence of CuZnSOD (50 U/mL) for 10 min. EPR sweep settings are described as in Materials and Methods section. The best fit for computer simulation was obtained with the following parameters: CYPMPO−OOH (a_N = 12.93 G, a_H = 10.97 G, a_P = 51.88 G, and line width value of 1.31 G) and CYPMPO−OH (a_N = 14.47 G, a_H = 13.50 G, a_P = 50.31 G, and line width value of 1.22 G).

buffer and experimental conditions used with mitochondria throughout the study.

Because of their slow reaction rates toward oxygen radicals, often high concentrations of nitrone spin-traps have been used for EPR spin-trapping of biological samples. Such high concentrations of spin-traps may have the unintentional consequence of inhibiting mitochondrial function, resulting in either an over- or underestimation of free radicals being produced. The effects of commonly used spin-traps on mitochondrial electron transport chain (ETC) activity were therefore examined. As shown in Figure 3, 10 mM CYPMPO, the concentration of spin-trap utilized throughout this study, had a minimal effect on NADH oxidase activity. In contrast, 50 mM DMPO and 25 mM DEPMPO inhibited NADH oxidase activity by 18.4% and 9.2%, respectively. These concentrations of DEPMPO and DMPO were the minimum concentrations required to obtain signals under our experimental settings. The extent of NADH oxidase inhibition by DMPO was concentration dependent, with 100 mM inhibiting activity by 65%. These results clearly indicate CYPMPO at concentrations required for spin-trap analysis has the least effect on mitochondrial electron transport chain activity.

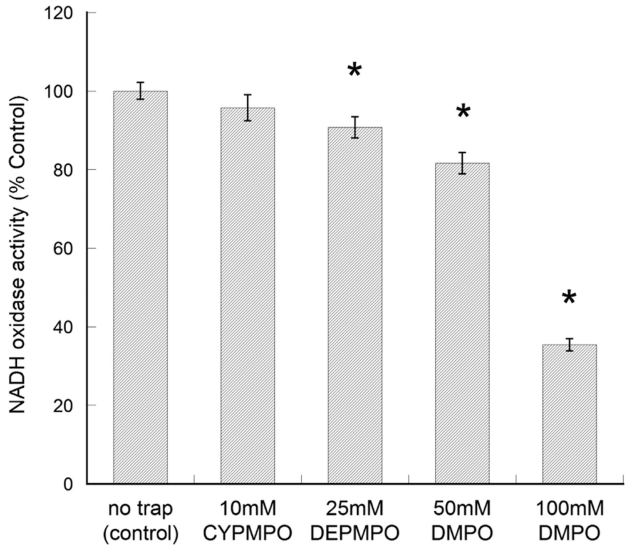

Figure 3. Inhibitory effect of nitrone spin-trapping agents on mitochondrial electron transport activity. NADH oxidase activity was measured spectrophotometrically as the rate at which SMPs at 25 μg/mL oxidized NADH (200 μM) in the absence or presence of indicated concentrations of spin-trapping agents. Values are expressed as percentages of the rates and are antimycin A inhibitable activities. Values represent means ± SD (n = 3). Asterisks indicate statistical significance ($p < 0.05$) using a Student t-test.

Measurements of Mitochondria Generating Free Radical Species. The detection of mitochondrial-derived free radicals was next determined using CYPMPO. For these experiments, we first examined the succinate-mediated (electron transfer through complexes II−III−IV) free radical production in submitochondrial particles (SMPs). SMPs were used to eliminate other potential sources of free radical generation and interference from endogenous antioxidants such as SOD2 (MnSOD). Under basal conditions, without ETC inhibitors, neither superoxide adduct nor hydroxyl radical adducts were observed after a 30 min incubation (Figure 4A). However, in the presence of the complex III-specific inhibitor, antimycin A, strong signals for superoxide adduct and minor signals for hydroxyl radical adduct were seen. Additional minor species were also observed (<10%) that may be attributable to semiquinone radicals.[6] Similar to the control X/XO system, the succinate-derived superoxide adduct peaks were abolished by exogenously supplied SOD (Figure 4A). Unlike the control X/XO experiment (Figure 2), though, the minor signals were also SOD sensitive. This may indicate the other observed radicals may be derived, in part, by the decomposition of superoxide adduct over time as reported for other nitrone spin-traps.[17−20]

In contrast to succinate, the NADH-mediated (electron transfer through complexes I−III−IV) free radical production in SMPs revealed more complex EPR spectra. As shown in Figure 4B, the NADH supplied SMPs did not generate observable superoxide adduct after a 30 min incubation. However, strong carbon-centered radical adduct peaks were produced, and these peaks were completely SOD insensitive. Surprisingly, even in the presence of the complex III inhibitor, antimycin A, superoxide adduct peaks were undetectable. However, antimycin A did enhance the intensity of the carbon-centered peaks. Similar stimulation of carbon-centered radical was detected with the complex I inhibitor rotenone (vide infra). The other species produced and identified by HFC constant

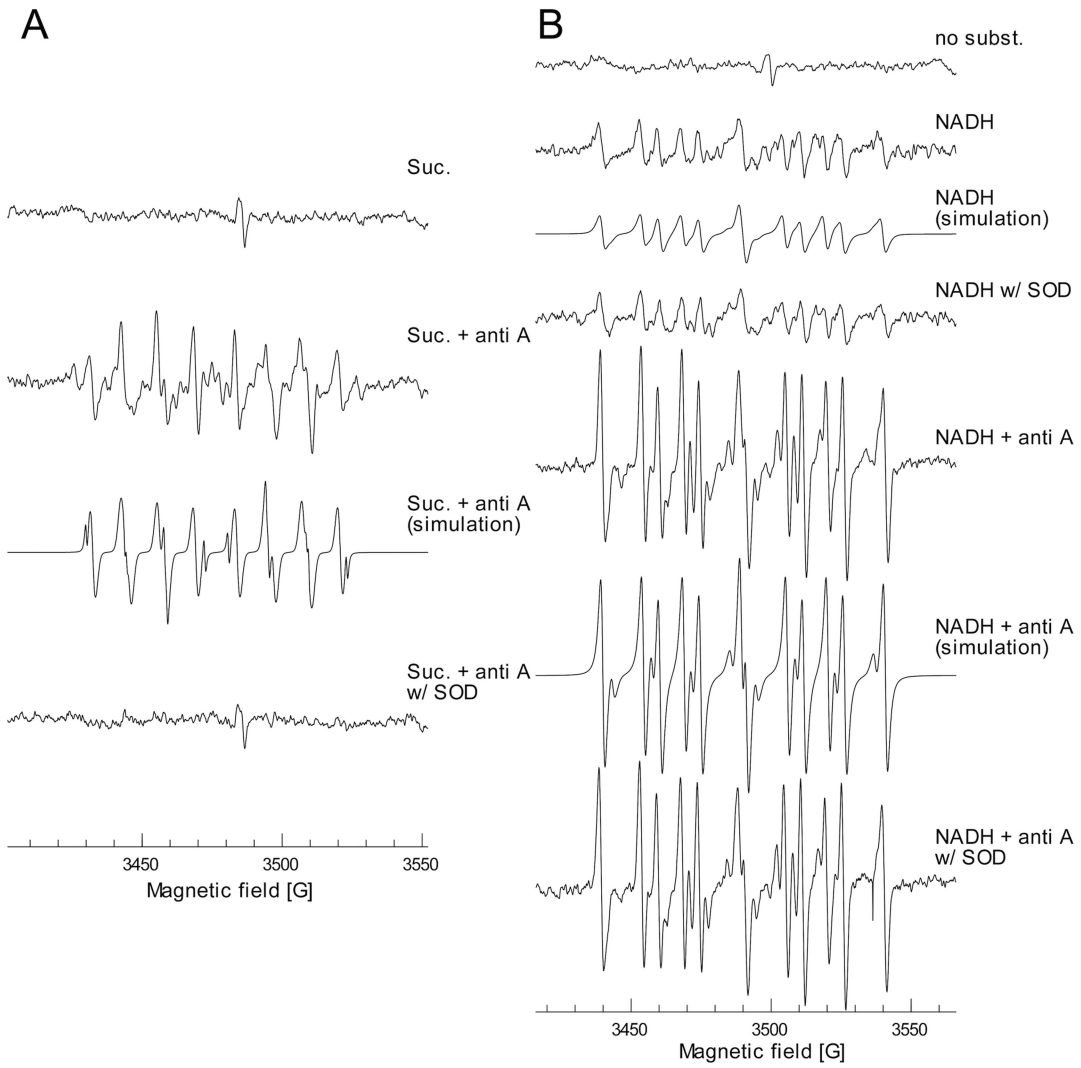

Figure 4. Mitochondria-mediated formation of CYPMPO adducts. EPR spectra were recorded after 30 min incubation of CYPMPO (10 mM) and 250 μg/mL SMPs supplemented with (A) 10 mM succinate or (B) 10 mM NADH, in 10 mM MOPS, 25 mM KCl, 1 mM EDTA, and 40 μM DTPA. Where indicated, CuZnSOD (50 U/mL) or antimycin A (200 nM) was incorporated. Computer simulation of the composite spectrum for succinate + antimycin A yielded ~91% CYPMPO−OOH (a_N = 12.94 G, a_H = 10.85 G, a_P = 51.60 G, and line width value of 1.07 G) and ~9% CYPMPO−OH (a_N = 14.32 G, a_H = 13.61 G, a_P = 50.56 G, and line width value of 0.88 G). Simulation for NADH (in the absence of inhibitor) showed 93.2% carbon-centered radical (a_N = 14.42 G, a_H = 20.65 G, a_P = 50.63 G, and line width value of 1.72 G) and 6.8% −OH adduct (a_N = 14.75 G, a_H = 14.02 G, a_P = 52.08 G, and line width value of 1.32 G). Similarly, simulation for NADH in the presence of antimycin A indicated 89.3% carbon-centered radical (a_N = 14.53 G, a_H = 20.43 G, a_P = 51.37 G, and line width value of 1.35 G) and 10.7% −OH adduct (a_N = 14.14 G, a_H = 14.08 G, a_P = 51.34 G, and line width value of 1.17 G).

were hydroxyl radical adducts. These results were somewhat unexpected, given the well-characterized capacity of NADH-driven respiration to generate superoxide. One possibility for the lack of superoxide detection is that CYPMPO might have a higher reaction rate toward the detected carbon-centered radical than to superoxide under neutral pH conditions. To test this hypothesis, we evaluated NADH-driven superoxide production in SMPs using a cyclic hydroxylamine spin-trap, 1-hydroxy-3-methoxycarbonyl-2,2,5,5-tetramethylpyrrolidine (CMH).[21] As shown in Figure 5, SMPs supplied with 10 mM NADH, 0.5 mM CMH, antimycin A, and under the same experimental conditions as with CYPMPO, SOD-sensitive superoxide production was observed. This superoxide-dependent signal increase was not affected by inclusion of 10 mM CYPMPO. This confirms that under the experimental conditions SMPs supplied with NADH produce superoxide anion. However, CYPMPO−OOH was not observed because of CYPMPO's preferential detection of carbon-centered radicals.

Experiments were next performed to determine whether the carbon-centered radicals were either membrane associated or soluble in origin. For these experiments, mitoplasts (disrupted mitochondria devoid of the outer membrane) were used because they could rapidly be partitioned into soluble and membrane fractions by low speed centrifugation. Importantly, mitoplasts also exhibit the same NADH-driven increase in carbon-centered radicals without apparent superoxide adducts. Fractionating mitoplasts into either soluble or membrane fractions after incubation with NADH and CYPMPO revealed that all of the detectable carbon-centered adduct population was in the supernatant (data not shown). This result suggests the observed carbon-centered radical is either a non-membrane associated protein or a small molecule.

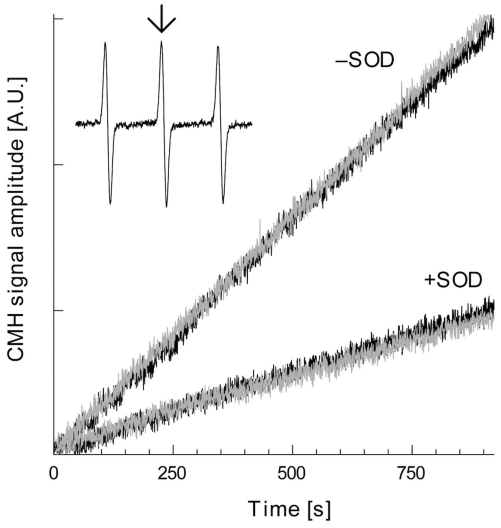

Figure 5. Measurement of mitochondrial superoxide production with CMH. Superoxide production kinetics were monitored by utilizing 25 μg/mL SMPs, 10 mM NADH, 200 nM antimycin A, and 500 μM CMH, in the absence and presence of 50 U/mL SOD1. The reaction was initiated in a flat cell in the cavity and peak intensity (indicated by arrow) was monitored over time. Black traces represent kinetics traces in the absence of CYPMPO and gray traces represent the presence of 10 mM CYPMPO.

The sensitivity of EPR spin-trapping experiments may actually be a detriment because detected radical species may be derived from contaminating metals or organic impurities that are present in the buffer or reagents. Several crucial experiments were therefore performed to address the potential contribution of carbon-centered radicals derived from non-mitochondrial sources and from experimental artifacts. First, it should be noted that all experiments were performed in the presence of chelators (40 μM DTPA and 1 mM EDTA utilized throughout this study) and that free radical production from free metal contamination within the buffer was largely mitigated. Second, identical mitochondria-derived carbon-centered radical adduct signals were obtained using 10 mM KH_2PO_4 instead of 10 mM MOPS, pH 7.4 (data not shown), thus demonstrating the products were not buffer type dependent. Finally, we also found that the NADH-driven carbon-centered radical production was not limited to detection by the CYPMPO spin-trap. We assessed EPR spin-trapping with two other more commonly employed nitrone-based traps (DEPMPO and BMPO) which are similar to CYPMPO but lack a six-membered ring. As shown in Figure 6, NADH supplied SMPs yielded comparable carbon-centered adduct signals with these spin-traps, which were completely distinguishable from X/XO-mediated superoxide adduct signals. Therefore, these experiments demonstrate the observed carbon-centered radical peaks are not artifacts of the buffer or chemistry unique to CYPMPO.

Assessment of Free Radical Species. The fractionation of the mitoplast reaction mixture demonstrated the origin of observed carbon-centered radical is either a non-membrane associated protein or a small molecule. Characterization of the NADH dependency of the carbon-centered radical formation therefore offered insights into the origin of the species. The signal intensity was found to be NADH concentration dependent in the presence of rotenone (Figure 7A), with carbon-centered radical detected with as little as 0.1 mM NADH. The concentration dependency of the signal suggests the carbon-centered radical may be originating on or from the dinucleotide. To further explore this hypothesis, we next examined the production of carbon-centered radicals utilizing a system that generates NADH rather than directly supplying the reduced dinucleotide. For these experiments, mitoplasts were supplied with glutamate, malate, and NAD^+. Endogenously present malate dehydrogenase (MDH) reduced the NAD^+ in the presence of malate, and glutamate served as a cosubstrate for removal of produced oxaloacetate by transamination. Figure 7B illustrates the behavior of adduct formation as NADH is produced by these reactions. In the absence of an ETC inhibitor, the endogenously produced NADH is quickly utilized by complex I, and hence carbon-centered radical formation was not observed. However, when antimycin A was included to allow for the accumulation of NADH, the carbon-centered radical adduct was then detected. Under these conditions, the steady-state concentration of 0.77 mM NADH was generated over a 30 min period from the reduction of NAD^+, as determined by measuring NADH's absorption peak (ε_{340} = 6220 M^{-1} cm^{-1}). In contrast, <30 μM NADH was produced in the absence of the ETC inhibitor (data not shown). This result demonstrates that accumulation of NADH drives the carbon-center radical formation and that NAD^+ alone cannot promote this reaction.

The requirement of NADH for the formation of the carbon-centered radical adduct raised the possibility that other NADH-requiring enzymes may also generate carbon-centered radical. To examine this possibility, the carbon-centered radical adduct formation was assessed in an in vitro system utilizing MDH (M1567; Sigma) as an enzymatic source of NADH oxidation. As shown in Figure 7C, NADH oxidation by MDH in the presence of oxaloacetate and CYPMPO did not yield carbon-centered radical adducts. This indicates that the formation of the carbon-centered radical is not a universal feature of enzymatic NADH oxidation.

The NADH concentration dependence on the formation of carbon-centered radical warranted further examination. Specifically, we sought further molecular evidence that the observed radical adduct originated from reduced dinucleotide. Experiments were performed in which an NADH analogue, nicotinamide mononucleotide (NMN; Figure 8A), was substituted for NADH. NMN is a precursor in the synthesis of NAD^+[22] and differs by the absence of adenosine monophosphate. As shown in Figure 8B, SMPs supplied with reduced NMN (NMNH) alone did not produce carbon-centered radical. This result was expected, given that NMNH does not serve as an electron donor to complex I. However, in the presence of NMNH and a catalytic amount of NADH (100 μM) to act as a redox initiator, equivalent carbon-centered radical adducts were detected. Similar results were obtained when NADPH, which is not a substrate of complex I at neutral pH, was substituted for NMNH (data not shown). These results demonstrate the contribution of NADH as the origin of carbon-centered radical and the dependence of reduced nicotinamide nucleotide moiety for propagation and accumulation of the adduct.

Mechanisms of NADH Radical Formation. The observed NADH radical may either be derived by, or a source of, reactive oxygen species. For example, even in the presence of chelators, there were detectable hydroxyl radical adduct peaks that could potentially contribute to the generation of other radical species. Therefore, we evaluated the kinetics of the

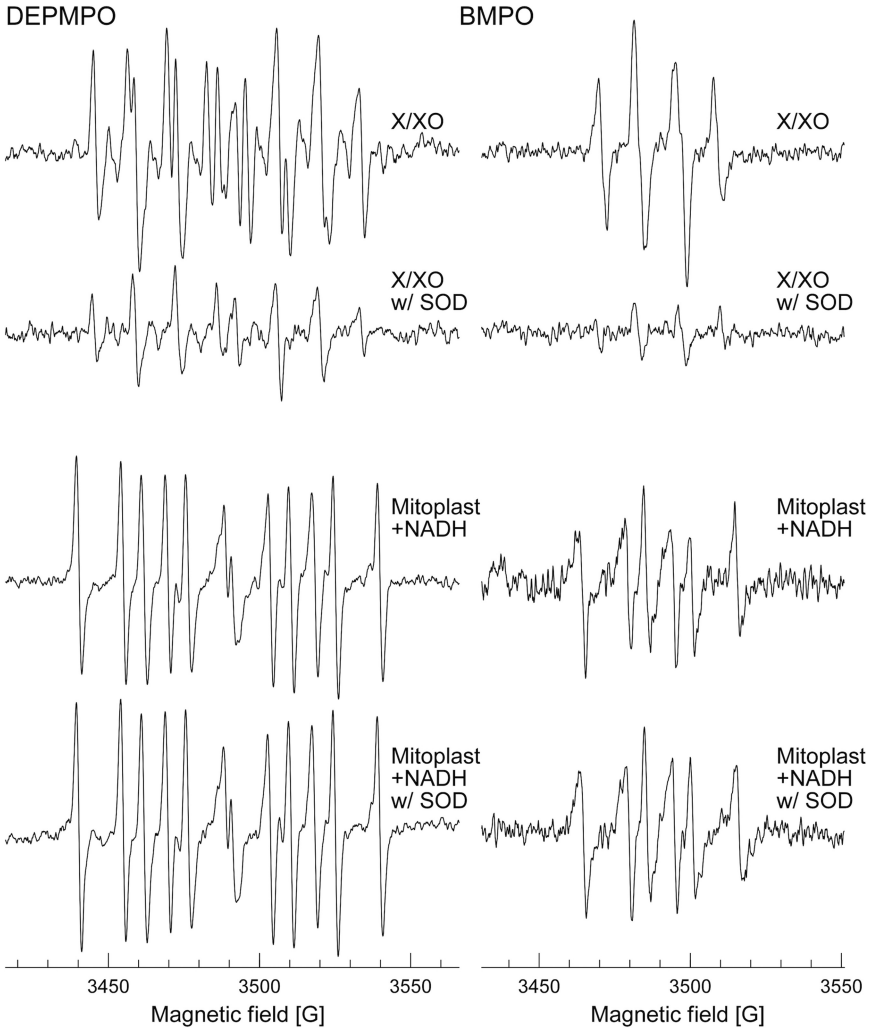

Figure 6. Comparison of EPR spectra of DEPMPO adducts and BMPO adducts. Upper panel: spectra were recorded after DEPMPO (25 mM) or BMPO (25 mM) were incubated with xanthine and xanthine oxidase in MOPS/EDTA/DTPA in the absence or presence of CuZnSOD for 10 min, as presented in Figure 2. Lower panel: DEPMPO (25 mM) or BMPO (25 mM) were incubated with 250 μg/mL SMPs supplemented with 10 mM NADH in the absence or presence of CuZnSOD for 30 min.

NADH radical adduct and the hydroxyl radical adduct formations to determine, in part, whether one species' production preceded the others. Figure 9A shows representative spectra of NADH supplemented SMPs with CYPMPO at two different time points, indicating the transient nature of hydroxyl radical adduct peaks. As characterized by HFC simulation of observed spectra, at the 10 min time point roughly 29% of total radical population was from hydroxyl radical species. However, by 30 min almost all (~96%) the signals were from the carbon-centered radical. The intensity change of these two species determined by 3 min incremental sweeps is traced in Figure 9B. Introduction of the hydroxyl radical scavenger dimethylthiourea (DMTU) suppressed both the hydroxyl radical and carbon-centered radical adduct formation (Figure 9B). Importantly, this result suggests the NADH-radical may be mediated or preceded by hydroxyl radicals.

We next evaluated the generation of the NADH adduct in a nonenzymatic hydroxyl radical generating system. As shown in Figure 10, brief exposure of UV to 50 mM H_2O_2 generated strong hydroxyl radical adduct peaks in the absence of NADH. H_2O_2 and NADH alone generated no detectable species. However, in the presence of NADH, H_2O_2, and UV exposure, carbon-centered radical adduct was now readily detected. The observed spectra were nearly identical with the carbon-centered radical detected in the mitochondrial systems. The NADH radical adduct peaks were completely abolished by the inclusion of DMTU. It is most likely that hydroxyl radicals extract the most reactive hydrogen in NADH, from the CH_2 group of ribose-nucleotide bridge (see Figure 8A for molecular structure), via nucleophilic substitution. These results further suggest hydroxyl radicals, generated in complex I, mediate the formation of NADH radical.

In contrast to hydroxyl radical, superoxide anion failed to generate the carbon-centered radical. Superoxide was generated in vitro by X/XO in the presence or absence of NADH. Even at the highest concentration of NADH tested (10 mM), formation of NADH radical was not detected (data not shown). From this result, together with the aforementioned SOD insensitivity, it is concluded the process of the NADH radical formation is a superoxide-independent process.

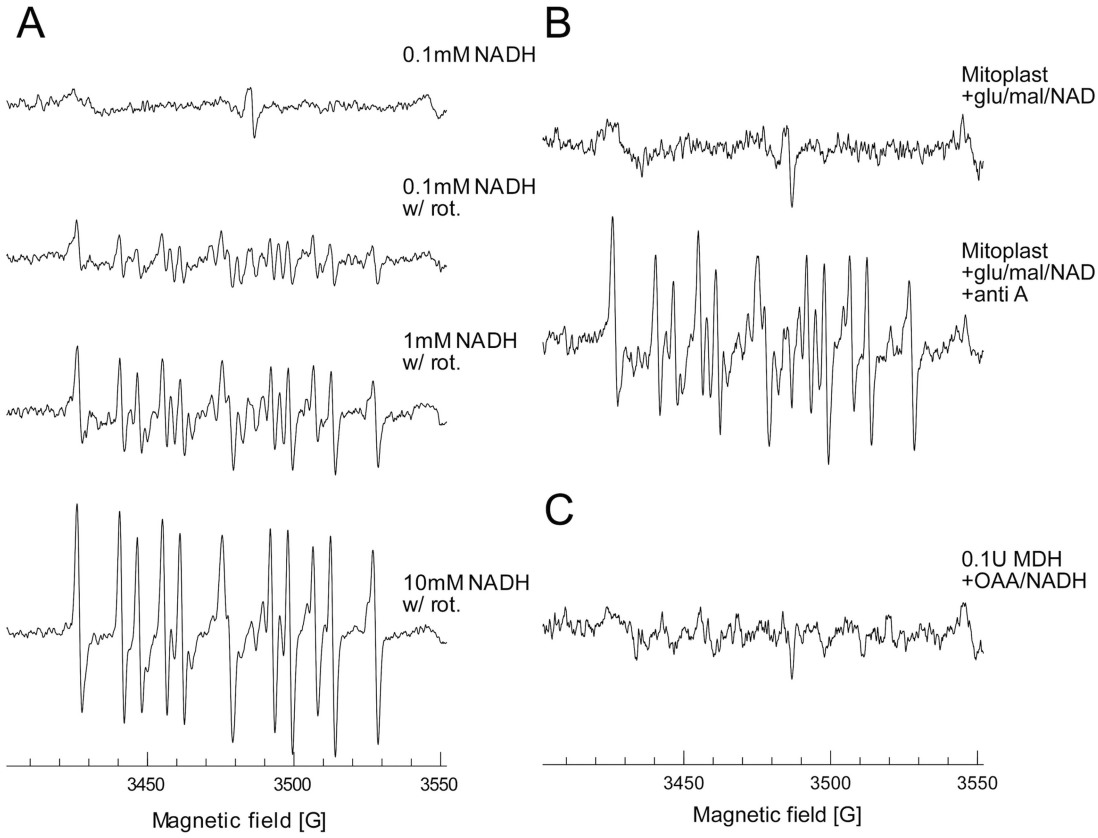

Figure 7. (A) NADH concentration dependency on carbon-centered radical formation. CYPMPO (10 mM) was incubated with 250 μg/mL mitoplasts and indicated concentration of NADH in the presence of complex I inhibitor rotenone (500 nM) for 30 min. (B) Carbon-centered radical formation by endogenous NADH production. EPR spectra were recorded after CYPMPO was incubated with 250 μg/mL mitoplasts, 10 mM glutamate, 2.5 mM malate, and 10 mM NAD^+, in the absence or presence of 200 nM antimycin A for 30 min. (C) Enzymatic oxidation of NADH is not sufficient for carbon-centered radical formation. Malate dehydrogenase (MDH; 0.1 U) was incubated with CYPMPO, oxaloacetate (1.0 mM) and NADH (10 mM) for 30 min.

DISCUSSION

This study employed the use of a recently described and commercially available spin-trap, CYPMPO, in detecting mitochondrial free radicals. As we demonstrate, this spin-trap has preferential qualities for use with mitochondria. Of particular significance, the concentration of CYPMPO required for free radical detection has less effect on mitochondrial ETC activity than commonly used spin-traps. Indeed, a dose-dependent inhibition of mitochondrial ETC activity was seen in the presence of concentrations of DMPO necessary for measuring radical adduct formation. It is known that inhibition of electron transport chain activity can have a positive or negative effect on free radical generation. Furthermore, small decreases in ETC activity can have a significant impact on free radical production.[13,23] Thus, the use of high concentrations of spin-traps may confound free radical measurements and may either under- or overestimate production.

The measurement of free radicals in mitochondrial preparation, either SMPs or mitoplasts, with CYPMPO revealed unexpected results. The most surprising observation was that SMPs or mitoplasts supplied with NADH produced little measurable superoxide anion, even in the presence of antimycin A, at physiological pH. Indeed, the major observed free radical species was a carbon-centered radical, which was readily identified by its unique HFC parameters and verified by simulation. As we demonstrated, the preferential detection of carbon-centered radical over superoxide in mitochondria supplied with NADH is likely a reflection of the relative reactivity of CYPMPO. Indeed, we were readily able to detect superoxide production in SMPs that were supplied with NADH and antimycin A using CMH. Detection of superoxide was sensitive to SOD but not to 10 mM CYPMPO. This preferential reaction of CYPMPO toward carbon-centered radicals was also found in SMPs supplied with both succinate and NADH in the presence of antimycin A. Separately, as presented in Figure 4, succinate and NADH generate superoxide and carbon-centered radical adducts, respectively. However, when both substrates are present, only the carbon-centered radical adduct signal was detected (not shown). These results strongly suggest the spin-trapping rate of CYPMPO is much greater toward carbon-centered radical species than toward superoxide at physiological pH.

Our results implicate the observed carbon-centered radical as an NADH radical adduct. This conclusion is supported by the observation that the intensity of the carbon-centered radical adduct peaks was NADH concentration dependent. However, NAD^+ or NADH oxidized by another dehydrogenase did not replicate the observed carbon-centered radical. Thus, the formation of this species is likely unique to electron transfer within complex I. In further support, we also demonstrated that mitochondria supplied with a catalytic amount of NADH and excess NMNH also gave rise to this radical adduct. This result suggests that the site of the radical is on the nicotinamide ribose portion of the dinucleotide, as NMNH lacks adenosine

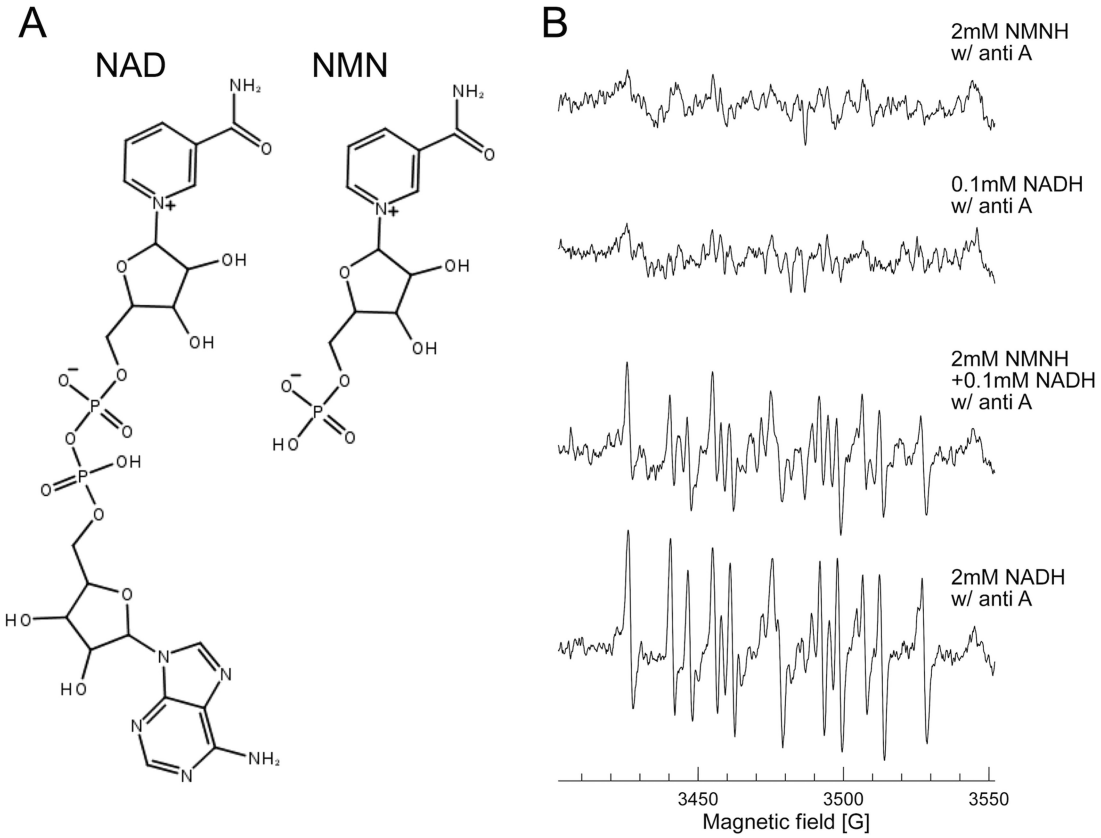

Figure 8. (A) Chemical structures of NAD^+ and nicotinamide mononucleotide (NMN). (B) Chemically reduced nicotinamide mononucleotide (NMNH) generates carbon-centered radical in the presence of catalytic amounts of NADH. EPR spectra were recorded after 10 mM CYPMPO was incubated with mitoplasts with 2 mM NMNH, 100 μM NADH, or 2 mM NMNH + 100 μM NADH for 30 min, all in the presence of antimycin A. For comparison purposes, the spectrum from CYPMPO incubated with 2 mM NADH is also presented.

phosphate. Based upon literature precedent, carbon-centered radicals spin-trapped by DEPMPO, characterized by 2.1 ± 0.1 mT HFC constants (a_H), were either alkyl or hydroxyalkyl radical adducts.[24−26] Under our experimental conditions, methyl radical adduct of CYPMPO generated by the reaction of UV/H_2O_2 with DMSO revealed a_H = 2.13 mT (not shown). This value is similar to our observed NADH-derived carbon-centered radical a_H value of 2.06 mT (Figure 4). Thus, we speculated our observed NADH radical adduct forms from the CH_2 group of ribose−nucleotide bridge of nicotinamide. Exact identification of the NADH radical adduct, attempted by LC/MS, was unsuccessful. The difficulty primarily arose from the limited stability of the adduct under conditions required for chromatographic separation. The development and implementation of new techniques, such as HPLC-EPR,[27−29] may facilitate the future identification of exact species.

While no previous report of a mitochondria-mediated NADH radical has been made, others have previously observed carbon-centered radicals in mitochondria.[1,7,30,31] Interestingly, the reported DMPO/DEPMPO spectra obtained under comparable experimental condition resemble our spectra of NADH radical adduct. However, in these previous studies the observed peaks were SOD sensitive, indicating different products and/or mechanisms than reported here. Recently, Lie et al. described the non-spin-trapped formation of the ubisemiquinone radical.[6] Their results implicated the short-lived semiquinone as a source of superoxide anion production. Under our experimental condition, however, formation of semiquinone is very unlikely because the carbon center radical observed was increased by rotenone, a type B complex I inhibitor and semiquinone antagonist.[32] There have also been numerous reports of carbon-centered or lipid radical formation with hemes (as in cytochromes) catalyzed by the introduction of *tert*-butyl hydroperoxide.[30,33−37] However, analysis of the HFC strength for EPR spin-traps can be inadequate for determining the exact species of organic molecular free radicals and protein-centered radicals. Therefore, to resolve exact species, the EPR spin-trapping technique conjunct with separation capability, such as LC and electrophoresis, or separate indirect chemical or biochemical approaches are required. Recently, for instance, the formation of cytochrome *c*-mediated tyrosyl radical has been resolved by the HPLC-EPR-MS technique.[38,39]

Another potential mitochondria-mediated carbon-centered radical adduct is CYPMPOX, a DMPOX-type aminoxyl radical. DMPOX (or CYPMPOX) forms either via direct oxidation of the spin-probe[40−42] or oxidation of hydroxyl radical adduct[43−45] in the presence of hydroperoxide. Recently, cytochrome *c*-mediated DMPOX formation in the presence of H_2O_2, or alternatively cytochrome *c*-mediated DMPO-OOH and $NAD^\bullet$ formation in the presence of NADH and H_2O_2, has been reported.[46] However, because of the following reasons, we conclude that the contribution of CYPMPOX adduct in our observed spectra is minimal. First, the recently reported HFC parameters for CYPMPOX[47] (a_N = 0.74 mT, a_H = 0.40, 0.33 mT, a_P = 3.93 mT) do not agree with our simulated HFC parameters for the carbon-centered radical (Figure 4B). Second, the stimulation in carbon-centered radical adduct

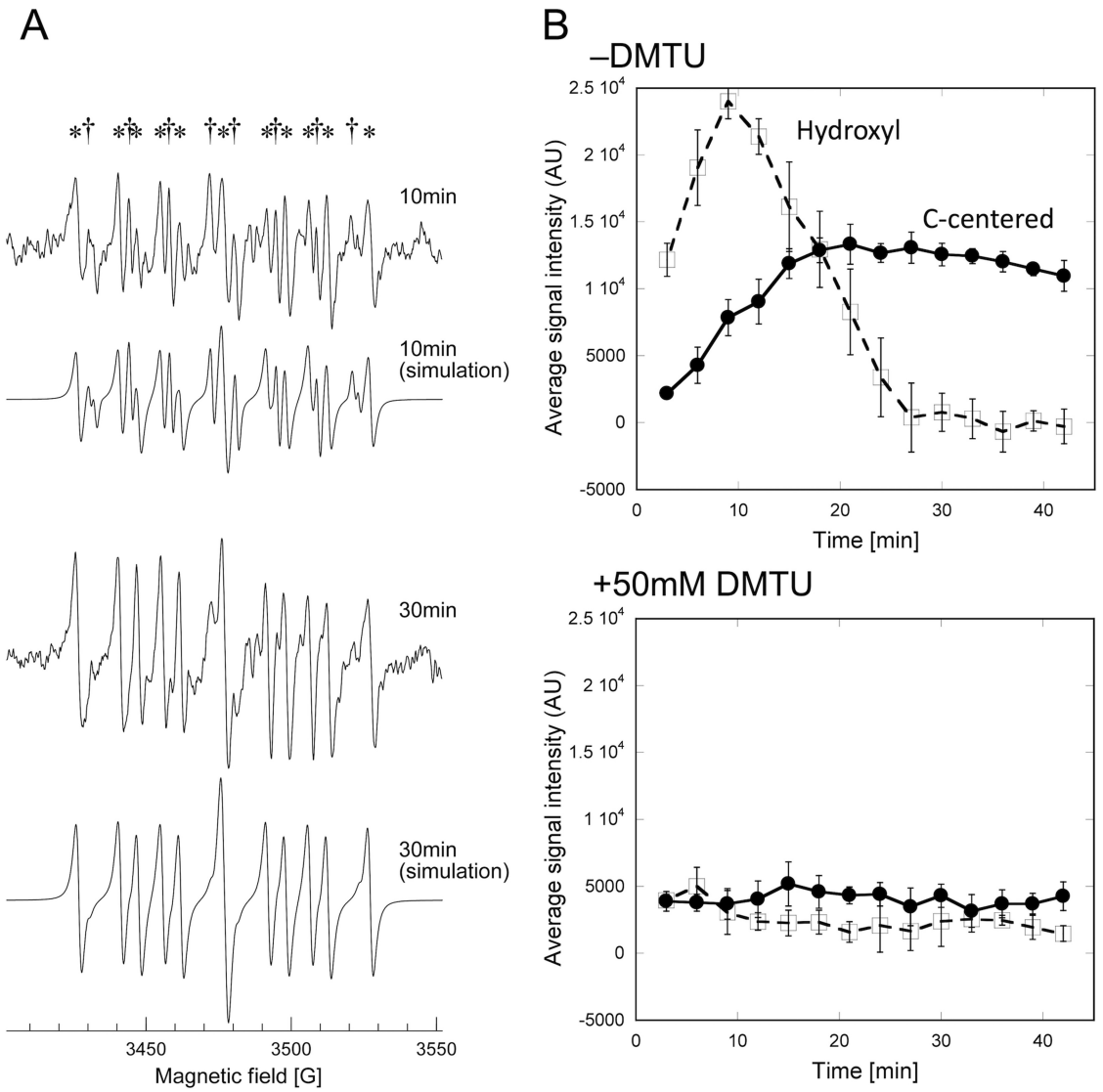

Figure 9. (A) Change in EPR spectral profile over time. EPR spectra were obtained after 10 and 30 min incubation of CYPMPO (10 mM), mitoplasts (250 μg/mL), and NADH (10 mM). Simulated spectrum for 10 min time-point consists of 71.0% carbon-centered radical (a_N = 14.45 G, a_H = 20.89 G, a_P = 50.78 G, and line width value of 1.57 G), 22.0% $-OH^1$ adduct diastereomer (a_N = 13.85 G, a_H = 14.37 G, a_P = 50.5 G, and line width value of 1.28 G), and 7.0% $-OH^2$ adduct diastereomer (a_N = 14.05 G, a_H = 12.30 G, a_P = 48.75 G, and line width value of 0.77 G). Simulation for 30 min time point is a composite of: 95.7% carbon-centered radical (a_N = 14.45 G, a_H = 20.68 G, a_P = 50.71 G, and line width value of 1.73 G) and 4.3% $-OH^1$ adduct (a_N = 13.99 G, a_H = 14.51 G, a_P = 51.0 G, and line width value of 1.41 G). Note that since the minor diastereomer species of hydroxyl adduct ($-OH^2$) quickly decomposes and was not observable in the 30 min time point, the contribution of $-OH^2$ in simulations for Figure 4 was omitted. (B) Kinetics of mitochondria-mediated carbon-centered radical adduct and hydroxyl adduct peaks. Series of EPR spectra were obtained by 3 min incremental sweeps. The average of peak intensities for each species, in the absence or presence of a hydroxyl radical scavenger DTMU (50 mM), is tabulated in terms of incubation time. The carbon-centered radical adduct peaks are denoted by the symbol ∗ and −OH adduct peaks labeled by the symbol † in 10 min time-point spectra in frame A. n = 4 per group.

formation in the presence of rotenone or antimycin A indicates it takes place far upstream of cytochrome *c*. It is possible though, because of the sensitivity or specificity of the probe and overlapping interference from other adducts' signals, that CYPMPOX adduct forms but is not observable under our experimental conditions.

In addition to the carbon-centered radical, we have also identified ETC-mediated hydroxyl radical formation. This ETC-mediated hydroxyl radical formation could perhaps be attributed to Haber−Weiss and Fenton reactions at the sites of metal complexes (Fe−S proteins, cytochromes, and Cu centers) via endogenously produced H_2O_2 formed by reduction of superoxide anion. Indeed, there have been reports that chelated and protein-bound Fe can participate in hydroxyl radical production.[48−50] However, SMPs are largely devoid of SOD2 and other antioxidants, thus impairing the production of H_2O_2 under our experimental condition. Nevertheless, SMPs produced observable hydroxyl radical adduct peaks (Figures 4 and 9) that were insensitive to exogenously supplied SOD. Although there is a paucity of evidence that complex I can directly and enzymatically generate hydroxyl radicals, the complex I inhibitor, MPP^+, has been shown to induce NADH dehydrogenase-mediated hydroxyl radical formation.[51,52] Indeed, our results are consistent with the hypothesis that the NADH radical formation is mediated by endogenously produced hydroxyl radicals. The fact that rotenone, a

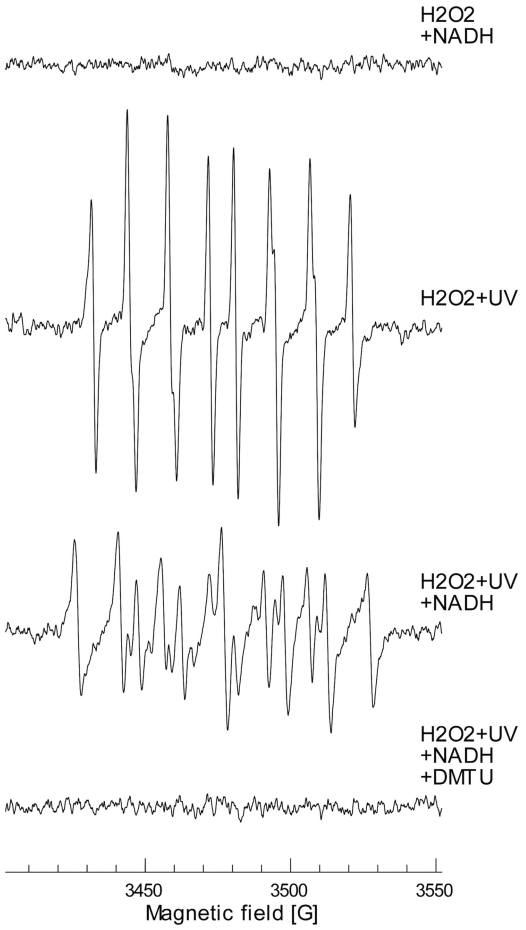

Figure 10. Nonenzymatic formation of NADH radicals. EPR spectra were recorded after 1.0 min exposure of UV radiation, as indicated, to a mixture containing CYPMPO (10 mM) and H_2O_2 (50 mM) in ddH_2O. As indicated, 10 mM NADH and/or 50 mM DMTU were included in the reaction mixture.

semiquinone antagonist, stimulated the NADH radical formation implicates a site of hydroxyl radical production that is upstream of the ubiquinone binding site, such as the FMN or Fe−S clusters within complex I.

The concentration of NADH in the matrix of heart mitochondria ranges from sub-millimolar up to ~3.5 mM concentrations.[53] Thus, the amount of NADH utilized in parts of this study (10 mM) was likely above physiological levels but required for certain aspects of this mechanistic study. For example, the high concentrations of NADH were necessary only to observe the NADH radical signal in the absence of ETC inhibitors. This is because the concentration of protein required to detect radical species quickly consumed sub-millimolar concentrations of NADH. However, in the presence of inhibitors (rotenone or antimycin A), a physiological concentration of NADH (100 μM) was sufficient for NADH radical production (Figure 7A).

A potential consequence of using high concentrations of NADH is that it may potentially react with, and mask, the detection of endogenously produced superoxide.[54,55] However, the reactivity of NADH toward superoxide has been reported <27 M^{-1} s^{-1}, whereas the rate constant for the reaction of hydroxyl radical with NADH has been shown to be 2×10^{10} M^{-1} s^{-1}.[56] To evaluate the superoxide scavenging capacity of NADH under our experimental conditions, superoxide was generated by X/XO in the presence or absence of 10 mM NADH. We found that this concentration of NADH had a moderate capacity to disrupt the formation of CYPMPO−OOH adduct signal. Importantly, though, this reaction did not yield carbon-centered radical, indicating superoxide is insufficient for catalyzing the NADH radicals.

The origin and consequence of carbon-centered or protein-centered radical formation in vivo are not well understood. They can be seen as intermediates of oxidative stress, damage that precedes other covalent modifications, or as sources of other free radicals. The downstream product of the NADH radical (in the absence of spin-traps) is yet to be determined. However, the decomposition of NADH radical may represent a potential secondary mechanism of complex I-mediated superoxide production upstream of the ubiquinone binding site (FMN site or Fe−S clusters). For example, an NAD^+ radical ($NAD^\bullet$) has been documented as a source of superoxide in in vitro systems (rate constant ~1.9×10^9 M^{-1} s^{-1}) in which $NAD^\bullet$ was generated by pulse radiolysis.[57,58] The physiological significance of $NAD^\bullet$ is unknown but has interesting implications as a potential source of mitochondrial superoxide. In addition, NADH also has high reactivity toward various free radical species such as thiyl or phenoxyl.[55] Thus, the NADH radical may not only be generated via different mechanisms and/or upstream intermediate radicals[59] but also may lead the production of secondary/tertiary free radical species in vivo. Moreover, the formation of NADH radicals or the interaction between the NADH radicals and nearby reactive proteins may also be important for redox based metabolic regulation. This is speculated based on the dependence of mitochondrial free radical formation on the NADH/NAD^+ ratio, which is also an important determinant in regulating numerous metabolic processes and the energetic status. These findings highlight the complexity of mitochondrial free radical production and demonstrate a radical species that may form even in the absence of oxygen. Clearly, these results demonstrate unappreciated radical species may form that perhaps have significance under normal and pathological conditions. Future studies aimed at identifying such species, as well as their mechanisms and sites of production, are warranted.

AUTHOR INFORMATION

Corresponding Author

*Phone: (405) 271-7584. Fax: (405) 271-1437. E-mail: Kenneth-Humphries@omrf.org.

Funding

This work was supported by a grant from the Oklahoma Center for Advancement of Science and Technology (HR09-139).

ABBREVIATIONS

BMPO, 5-*tert*-butoxycarbonyl-5-methyl-1-pyrroline *N*-oxide; CMH, 1-hydroxy-3-methoxycarbonyl-2,2,5,5-tetramethylpyrrolidine; CYPMPO, 5-(2,2-dimethyl-1,3-propoxycyclophosphoryl)-5-methyl-1-pyrroline *N*-oxide; DEPMPO, 5-(diethoxyphosphoryl)-5-methyl-1-pyrroline *N*-oxide; DMPO, 5,5-dimethyl-1-pyrroline *N*-oxide; DMTU, dimethylthiourea; DTPA, diethylenetriaminepentaacetic acid; EDTA, ethylenediaminetetraacetic acid; EPR, electron paramagnetic resonance; ETC, electron transport chain; HFC, hyperfine coupling; MOPS, 3-(*N*-morpholino)propanesulfonic acid; NAD^+/NADH, nicotinamide adenine dinucleotide (oxidized/reduced); NMN,

nicotinamide mononucleotide; SOD, superoxide dismutase; SMP, submitochondrial particle.

REFERENCES

(1) Ali, S. S., Marcondes, M. C., Bajova, H., Dugan, L. L., and Conti, B. (2010) Metabolic depression and increased reactive oxygen species production by isolated mitochondria at moderately lower temperatures. *J. Biol. Chem. 285*, 32522−32528.

(2) Hruszkewycz, A. M., and Bergtold, D. S. (1990) The 8-hydroxyguanine content of isolated mitochondria increases with lipid peroxidation. *Mutat. Res. 244*, 123−128.

(3) Long, J., Gao, H., Sun, L., Liu, J., and Zhao-Wilson, X. (2009) Grape extract protects mitochondria from oxidative damage and improves locomotor dysfunction and extends lifespan in a Drosophila Parkinson's disease model. *Rejuvenation Res. 12*, 321−331.

(4) Dykens, J. A. (1994) Isolated Cerebral and Cerebellar Mitochondria Produce Free Radicals when Exposed to Elevated Ca2+ and Na+: Implications for Neurodegeneration. *J. Neurochem. 63*, 584−591.

(5) Grijalba, M. T., Vercesi, A. E., and Schreier, S. (1999) Ca2+-Induced Increased Lipid Packing and Domain Formation in Submitochondrial Particles. A Possible Early Step in the Mechanism of Ca2+-Stimulated Generation of Reactive Oxygen Species by the Respiratory Chain†. *Biochemistry 38*, 13279−13287.

(6) Liu, Y., Zhao, H., Li, H., Kalyanaraman, B., Nicolosi, A. C., and Gutterman, D. D. (2003) Mitochondrial sources of H2O2 generation play a key role in flow-mediated dilation in human coronary resistance arteries. *Circ. Res. 93*, 573−580.

(7) Fang, J., and Beattie, D. S. (2003) External alternative NADH dehydrogenase of Saccharomyces cerevisiae: a potential source of superoxide. *Free Radical Biol. Med. 34*, 478−488.

(8) Hauptmann, N., Grimsby, J., Shih, J. C., and Cadenas, E. (1996) The Metabolism of Tyramine by Monoamine Oxidase A/B Causes Oxidative Damage to Mitochondrial DNA. *Arch. Biochem. Biophys. 335*, 295−304.

(9) Bartosz, G. (2006) Use of spectroscopic probes for detection of reactive oxygen species. *Clin. Chim. Acta 368*, 53−76.

(10) Khan, N., Wilmot, C. M., Rosen, G. M., Demidenko, E., Sun, J., Joseph, J., O'Hara, J., Kalyanaraman, B., and Swartz, H. M. (2003) Spin traps: in vitro toxicity and stability of radical adducts. *Free Radical Biol. Med. 34*, 1473−1481.

(11) Saito, K., Takahashi, M., Kamibayashi, M., Ozawa, T., and Kohno, M. (2009) Comparison of superoxide detection abilities of newly developed spin traps in the living cells. *Free Radical Res. 43*, 668−676.

(12) Kamibayashi, M., Oowada, S., Kameda, H., Okada, T., Inanami, O., Ohta, S., Ozawa, T., Makino, K., and Kotake, Y. (2006) Synthesis and characterization of a practically better DEPMPO-type spin trap, 5-(2,2-dimethyl-1,3-propoxy cyclophosphoryl)-5-methyl-1-pyrroline N-oxide (CYPMPO). *Free Radical Res. 40*, 1166−1172.

(13) Adam-Vizi, V. (2005) Production of reactive oxygen species in brain mitochondria: contribution by electron transport chain and non-electron transport chain sources. *Antioxid. Redox Signaling 7*, 1140−1149.

(14) Murphy, M. P. (2009) How mitochondria produce reactive oxygen species. *Biochem. J. 417*, 1−13.

(15) Matsuzaki, S., and Szweda, L. I. (2007) Inhibition of complex I by Ca2+ reduces electron transport activity and the rate of superoxide anion production in cardiac submitochondrial particles. *Biochemistry 46*, 1350−1357.

(16) Duling, D. R. (1994) Simulation of multiple isotropic spin-trap EPR spectra. *J. Magn. Reson., Ser. B 104*, 105−110.

(17) Finkelstein, E., Rosen, G. M., and Rauckman, E. J. (1982) Production of hydroxyl radical by decomposition of superoxide spin-trapped adducts. *Mol. Pharmacol. 21*, 262−265.

(18) Lauricella, R., Allouch, A., Roubaud, V., Bouteiller, J.-C., and Tuccio, B. (2004) A new kinetic approach to the evaluation of rate constants for the spin trapping of superoxide/hydroperoxyl radical by nitrones in aqueous media. *Org. Biomol. Chem. 2*, 1304−1309.

(19) Lloyd, R. V., and Mason, R. P. (1990) Evidence against transition metal-independent hydroxyl radical generation by xanthine oxidase. *J. Biol. Chem. 265*, 16733−16736.

(20) Villamena, F. A. (2009) Superoxide radical anion adduct of 5,5-dimethyl-1-pyrroline N-oxide. 5. Thermodynamics and kinetics of unimolecular decomposition. *J. Phys. Chem. A 113*, 6398−6403.

(21) Dikalov, S. I., Kirilyuk, I. A., Voinov, M., and Grigor'ev, I. A. (2011) EPR detection of cellular and mitochondrial superoxide using cyclic hydroxylamines. *Free Radical Res. 45*, 417−430.

(22) Belenky, P., Racette, F. G., Bogan, K. L., McClure, J. M., Smith, J. S., and Brenner, C. (2007) Nicotinamide riboside promotes Sir2 silencing and extends lifespan via Nrk and Urh1/Pnp1/Meu1 pathways to NAD+. *Cell 129*, 473−484.

(23) Matsuzaki, S., Szweda, L. I., and Humphries, K. M. (2009) Mitochondrial superoxide production and respiratory activity: biphasic response to ischemic duration. *Arch. Biochem. Biophys. 484*, 87−93.

(24) Khramtsov, V., Berliner, L. J., and Clanton, T. L. (1999) NMR spin trapping: Detection of free radical reactions using a phosphorus-containing nitrone spin trap. *Magn. Reson. Med. 42*, 228−234.

(25) Maury, J., Feray, L., Bazin, S., Clément, J.-L., Marque, S. R. A., Siri, D., and Bertrand, M. P. (2011) Spin-Trapping Evidence for the Formation of Alkyl, Alkoxyl, and Alkylperoxyl Radicals in the Reactions of Dialkylzincs with Oxygen. *Chem.—Eur. J. 17*, 1586−1595.

(26) Culcasi, M., Muller, A., Mercier, A., Clément, J.-L., Payet, O., Rockenbauer, A., Marchand, V., and Pietri, S. (2006) Early specific free radical-related cytotoxicity of gas phase cigarette smoke and its paradoxical temporary inhibition by tar: An electron paramagnetic resonance study with the spin trap DEPMPO. *Chem.-Biol. Interact. 164*, 215−231.

(27) Chen, Y.-R. (2008) EPR Spin-Trapping and Nano LC MS/MS Techniques for DEPMPO/[•]OOH and Immuno-spin-Trapping with Anti-DMPO Antibody in Mitochondrial Electron Transfer System, in *Advanced Protocols in Oxidative Stress I* (Armstrong, D., Ed.) pp 75−88, Humana Press, New York.

(28) Iwahashi, H. (2008) High Performance Liquid Chromatography/Electron Spin Resonance/Mass Spectrometry Analyses of Lipid-Derived Radicals, in *Advanced Protocols in Oxidative Stress I* (Armstrong, D., Ed.) pp 65−73, Humana Press, New York.

(29) Kumamoto, K., Hirai, T., Kishioka, S., and Iwahashi, H. (2007) Identification of a radical formed in the reaction mixture of rat brain homogenate with a ferrous ion/ascorbic acid system using HPLC-EPR and HPLC-EPR-MS. *Free Radical Res. 41*, 650−654.

(30) Massa, E. M., and Giulivi, C. (1993) Alkoxyl and methyl radical formation during cleavage of tert-butyl hydroperoxide by a mitochondrial membrane-bound, redox active copper pool: an EPR study. *Free Radical Biol. Med. 14*, 559−565.

(31) Kennedy, C. H., Church, D. F., Winston, G. W., and Pryor, W. A. (1992) tert-Butyl hydroperoxide-induced radical production in rat liver mitochondria. *Free Radical Biol. Med. 12*, 381−387.

(32) Degli Esposti, M. (1998) Inhibitors of NADH-ubiquinone reductase: an overview. *Biochim. Biophys. Acta 1364*, 222−235.

(33) Rota, C., Barr, D. P., Martin, M. V., Guengerich, F. P., Tomasi, A., and Mason, R. P. (1997) Detection of free radicals produced from the reaction of cytochrome P-450 with linoleic acid hydroperoxide. *Biochem. J. 328* (Pt 2), 565−571.

(34) Davies, M. J. (1989) Detection of peroxyl and alkoxyl radicals produced by reaction of hydroperoxides with rat liver microsomal fractions. *Biochem. J. 257*, 603−606.

(35) Chamulitrat, W., Takahashi, N., and Mason, R. P. (1989) Peroxyl, alkoxyl, and carbon-centered radical formation from organic hydroperoxides by chloroperoxidase. *J. Biol. Chem. 264*, 7889−7899.

(36) Kalyanaraman, B., Mottley, C., and Mason, R. P. (1983) A direct electron spin resonance and spin-trapping investigation of peroxyl free radical formation by hematin/hydroperoxide systems. *J. Biol. Chem. 258*, 3855−3858.

(37) Barr, D. P., and Mason, R. P. (1995) Mechanism of radical production from the reaction of cytochrome c with organic hydroperoxides. An ESR spin trapping investigation. *J. Biol. Chem. 270*, 12709−12716.

(38) Gunther, M. R., Tschirret-Guth, R. A., Witkowska, H. E., Fann, Y. C., Barr, D. P., Ortiz De Montellano, P. R., and Mason, R. P. (1998) Site-specific spin trapping of tyrosine radicals in the oxidation of metmyoglobin by hydrogen peroxide. *Biochem. J. 330* (Pt 3), 1293−1299.
(39) Qian, S. Y., Chen, Y. R., Deterding, L. J., Fann, Y. C., Chignell, C. F., Tomer, K. B., and Mason, R. P. (2002) Identification of protein-derived tyrosyl radical in the reaction of cytochrome c and hydrogen peroxide: characterization by ESR spin-trapping, HPLC and MS. *Biochem. J. 363*, 281−288.
(40) Mao, G. D., Thomas, P. D., and Poznansky, M. J. (1994) Oxidation of spin trap 5,5-dimethyl-1-pyrroline-1-oxide in an electron paramagnetic resonance study of the reaction of methemoglobin with hydrogen peroxide. *Free Radical Biol. Med. 16*, 493−500.
(41) Floyd, R. A., and Soong, L. M. (1977) Spin trapping in biological systems. Oxidation of the spin trap 5,5-dimethyl-1-pyrroline-1-oxide by a hydroperoxide-hematin system. *Biochem. Biophys. Res. Commun. 74*, 79−84.
(42) Finkelstein, E., Rosen, G. M., and Rauckman, E. J. (1980) Spin trapping of superoxide and hydroxyl radical: practical aspects. *Arch. Biochem. Biophys. 200*, 1−16.
(43) Bernofsky, C., Bandara, B. M., and Hinojosa, O. (1990) Electron spin resonance studies of the reaction of hypochlorite with 5,5-dimethyl-1-pyrroline-N-oxide. *Free Radical Biol. Med. 8*, 231−239.
(44) Rosen, G. M., and Rauckman, E. J. (1980) Spin trapping of the primary radical involved in the activation of the carcinogen N-hydroxy-2-acetylaminofluorene by cumene hydroperoxide-hematin. *Mol. Pharmacol. 17*, 233−238.
(45) Jones, C. M., and Burkitt, M. J. (2002) EPR detection of the unstable tert-butylperoxyl radical adduct of the spin trap 5,5-dimethyl-1-pyrroline N-oxide: a combined spin-trapping and continuous-flow investigation. *J. Chem. Soc., Perkin Trans. 2*, 2044−2051.
(46) Velayutham, M., Hemann, C., and Zweier, J. L. (2011) Removal of H(2)O(2) and generation of superoxide radical: Role of cytochrome c and NADH. *Free Radical Biol. Med. 51*, 160−170.
(47) Nakajima, A., Matsuda, E., Ueda, Y., and Tajima, K. (2010) ESR analysis of the oxidation reactions of phosphorus-containing nitrone-type spin traps with gold(III) ion. *Can. J. Chem. 88*, 556−562.
(48) Miller, D. M., Buettner, G. R., and Aust, S. D. (1990) Transition metals as catalysts of "autoxidation" reactions. *Free Radical Biol. Med. 8*, 95−108.
(49) Minotti, G., and Aust, S. D. (1989) The role of iron in oxygen radical mediated lipid peroxidation. *Chem.-Biol. Interact. 71*, 1−19.
(50) Tien, M., Morehouse, L. A., Bucher, J. R., and Aust, S. D. (1982) The multiple effects of ethylenediaminetetraacetate in several model lipid peroxidation systems. *Arch. Biochem. Biophys. 218*, 450−458.
(51) Adams, J. D. Jr, Klaidman, L. K., and Leung, A. C. (1993) MPP+ and MPDP+ induced oxygen radical formation with mitochondrial enzymes. *Free Radical Biol. Med. 15*, 181−186.
(52) Chiueh, C. C., Krishna, G., Tulsi, P., Obata, T., Lang, K., Huang, S.-J., and Murphy, D. L. (1992) Intracranial microdialysis of salicylic acid to detect hydroxyl radical generation through dopamine autooxidation in the caudate nucleus: Effects of MPP+. *Free Radical Biol. Med. 13*, 581−583.
(53) Blinova, K., Carroll, S., Bose, S., Smirnov, A. V., Harvey, J. J., Knutson, J. R., and Balaban, R. S. (2005) Distribution of Mitochondrial NADH Fluorescence Lifetimes: Steady-State Kinetics of Matrix NADH Interactions. *Biochemistry 44*, 2585−2594.
(54) Chan, P. C., and Bielski, B. H. (1974) Enzyme-catalyzed free radical reactions with nicotinamide adenine nucleotides. II. Lactate dehydrogenase-catalyzed oxidation of reduced nicotinamide adenine dinucleotide by superoxide radicals generated by xanthine oxidase. *J. Biol. Chem. 249*, 1317−1319.
(55) Olek, R. A., Ziolkowski, W., Kaczor, J. J., Greci, L., Popinigis, J., and Antosiewicz, J. (2004) Antioxidant activity of NADH and its analogue--an in vitro study. *J. Biochem. Mol. Biol. 37*, 416−421.
(56) Goldstein, S., and Czapski, G. (2000) Reactivity of peroxynitrite versus simultaneous generation of (*)NO and O(2)(*)(-) toward NADH. *Chem. Res. Toxicol. 13*, 736−741.
(57) Bielski, B. H. J., and Chan, P. C. (1980) Studies on free and enzyme-bound nicotinamide adenine dinucleotide free radicals. *J. Am. Chem. Soc. 102*, 1713−1716.
(58) Willson, R. L. (1970) Pulse radiolysis studies of electron transfer reactions in aerobic solution. *J. Chem. Soc. D*, 1005−1005.
(59) Forni, L. G., and Willson, R. L. (1986) Thiyl and phenoxyl free radicals and NADH. Direct observation of one-electron oxidation. *Biochem. J. 240*, 897−903.